

Laser induced photodissociation of stetrizine probed by photoelectron spectroscopy with synchrotron radiation

Laurent Nahon, Paul Morin, Michel Larzilliere, and Irene Nenner

Citation: *The Journal of Chemical Physics* **96**, 3628 (1992); doi: 10.1063/1.461916

View online: <http://dx.doi.org/10.1063/1.461916>

View Table of Contents: <http://scitation.aip.org/content/aip/journal/jcp/96/5?ver=pdfcov>

Published by the [AIP Publishing](#)

Articles you may be interested in

[Threshold photoelectron spectroscopy using synchrotron radiation](#)

AIP Conf. Proc. **576**, 703 (2001); 10.1063/1.1395405

[Ultraviolet photodissociation of furan probed by tunable synchrotron radiation](#)

J. Chem. Phys. **111**, 100 (1999); 10.1063/1.479257

[Atomic spectroscopy with laser and synchrotron radiation](#)

AIP Conf. Proc. **258**, 18 (1992); 10.1063/1.42523

[Auger photoelectron coincidence spectroscopy using synchrotron radiation](#)

Rev. Sci. Instrum. **63**, 3013 (1992); 10.1063/1.1142602

[Photoelectron microscopy and spectroscopy using synchrotron radiation](#)

J. Vac. Sci. Technol. A **9**, 1634 (1991); 10.1116/1.577477



Laser induced photodissociation of *s*-tetrazine probed by photoelectron spectroscopy with synchrotron radiation

Laurent Nahon

LURE, Laboratoire mixte CEA, CNRS et MEN, Université Paris Sud, Bât. 209D, 91405 Orsay Cedex France and X-Recherche Service, PARC-CLUB, 28 rue Jean Rostand 91893 Orsay Cedex France

Paul Morin

LURE, Laboratoire mixte CEA, CNRS et MEN, Université Paris Sud, Bât. 209D, 91405 Orsay Cedex France and CEA, CEN Saclay, Département d'Etude sur l'Etat Condensé, les Atomes et les Molécules, Service des Photons, Atomes et Molécules, 91191 Gif sur Yvette Cedex France

Michel Larzilliere

Laboratoire de Physique Atomique et Moléculaire, Université Laval, Québec, QC G1K 7P4, Canada

Irene Nenner

LURE, Laboratoire mixte, CEA, CNRS et MEN, Université Paris Sud, Bât. 209D, 91405 Orsay Cedex France and CEA, CEN Saclay, Département d'Etude sur l'Etat Condensé, les Atomes et les Molécules, Service des Photons, Atomes et Molécules, 91191 Gif sur Yvette Cedex France

(Received 26 June 1991; accepted 29 November 1991)

We have combined a cw visible laser with synchrotron radiation, respectively, to photodissociate the *s*-tetrazine molecule and to probe, with an electron analyzer, the vibrational energy of the nascent fragments. No fragments other than N₂ and HCN were detected on the time scale of our experiment. We find that 5.4% ± 0.5% of the nitrogen fragment departs with one quantum of vibration and at least 26% of each HCN fragment is vibrationally excited, mainly in the bending mode ($n = 1$ to 6) and probably to a very small extent in the C–N stretching mode ($n = 1$). These data are fully consistent with a pure three body fragmentation mechanism governed by the geometry of the transition state as calculated by Scheiner *et al.*, J. Am. Chem. Soc. **108**, 8160 (1986).

I. INTRODUCTION

The photodissociation of ground state *s*-tetrazine, near the S_1 state, with visible light, into three bodies, i.e., one N₂ and two HCN molecules, has raised considerable interest since the early work of Curtius *et al.*,¹ Koenigsberger and Vogt,² and later Hochstrasser and King.³ This process is strongly exothermic, as shown in Fig. 1, and provides an interesting case, which perhaps cannot be described with statistical models. The central question concerns the dissociation mechanism itself. Several experimental studies^{4–7} including the most recent ones, have discussed the occurrence of a concerted triple fragmentation



and sequential two body fragmentation processes



Except the work of Glowia and Riley⁶ who found evidence of a double translational energy distribution of HCN and favored process (2), any of the recent experimental work tend to prove a concerted triple fragmentation (1) along a repulsive surface. Coulter *et al.*,⁵ using time resolved fluorescence found very little vibrational excitation in the fragment, namely, 1% in the C–N stretching mode (ν_3) a negligible amount in the C–H stretching mode (ν_1) of HCN, and they estimated some 10% in N₂. Note that there is no experiment reported, to our knowledge, on the excitation of the bending mode in HCN. Zhao *et al.*⁷ on the basis of

photofragment translational spectroscopy measurements, reported that 73.9% of the available energy is found in translation, thus confirming that little internal energy is left in the fragments. Furthermore, the same authors measured an anisotropy in this dissociation, showing a stronger repulsion between the two HCN compared to the repulsion between HCN and N₂.

Meanwhile, *ab initio* molecular structure calculations⁸ have shown that the activation energy for the three body fragmentation is low (47 kcal/mol) enough to make this

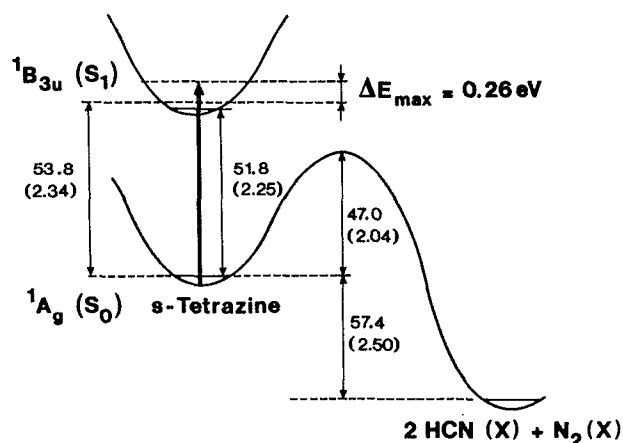


FIG. 1. Energy diagram of *s*-tetrazine photodissociation with energies in kcal/mol and in eV in parentheses, from Ref. 7.

route energetically open after $S_0 \rightarrow S_1$ photoexcitation (see Fig. 1). More recently, Strauss and Houston⁹ have proposed a method to appreciate the difference between a concerted mechanism and a stepwise process. On the basis of the interpretation of the fragment translational distribution and the anisotropy of the fragmentation of *s*-tetrazine, measured by Zhao *et al.*,⁷ they concluded to a synchronous and concerted mechanism. The question of the complete partitioning of vibrational and rotational excitation among the fragments remains open, in order to approach the dynamics of this fragmentation.

In this paper, we report novel measurements on this photodissociation problem, by probing in the gas phase, the nature and the detailed vibrational energy content of the fragments by photoelectron spectroscopy. This method has been already proved to be well adapted for studying unstable molecules,^{10,11} chemical reactions in the gas phase (also called chemielectron spectroscopy) such as metal oxidation reactions¹² or pyrolysis of azides.¹³ Here we introduce two novel aspects:¹⁴ One is the use of synchrotron radiation in the vacuum ultraviolet, at selected wavelengths, in order to maximize the sensitivity according to the nature of the products to be probed. Another is to use this method to the specific problem of state to state laser molecular photodissociation. Actually, we have built an experimental setup¹⁵ and used it for studying the ionization of open shell species such as iodine atoms¹⁶ produced by photodissociation of the I_2 molecule. In the present paper, we focus our attention on the laser induced dissociation process, in probing the fragments by photoelectron spectroscopy. Regarding the problem of fragmentation of *s*-tetrazine photoexcited near the S_1 state, we identify the nature of the fragments N_2 and HCN, and the distribution of their vibrational energy. The present results are found compatible with a concerted triple fragmentation process, after a $S_1 \rightarrow S_0$ internal conversion, as suggested by Zhao *et al.*⁷ We show that the geometrical structure of the transition state, calculated by Scheiner *et al.*⁸ governs the vibrational excitation along the various coordinates of the fragments. Further insights on the dynamics of this fragmentation are discussed.

II. EXPERIMENT

The experimental setup and procedure have been described in details previously,^{15,16} and will be presented here briefly. Synchrotron radiation emitted from the Super ACO (Super Anneau de Collisions d'Orsay) positron storage ring, is monochromatized by a 2.5 m toroidal grating monochromator. The synchrotron light wavelength is selected in the vacuum ultraviolet (vuv) region around 23 eV photon energy, with a bandwidth of about 60 meV. This energy corresponds to the maximum of photoionization cross section of N_2 in the N_2^+ , $A(^2\Pi_u)$ state,¹⁷ which is well suited for detecting hot vibrational bands. Note that this energy is also adequate for detecting HCN. The monochromatic beam is refocused by a toroidal platinum coated mirror into the center of the experimental chamber. The photon flux at 23 eV, amounts to 3×10^{11} photon/s⁻¹ per 40 meV bandwidth.

A schematic of the experimental setup is shown in Fig. 2. The vuv light beam crosses the interaction zone, formed

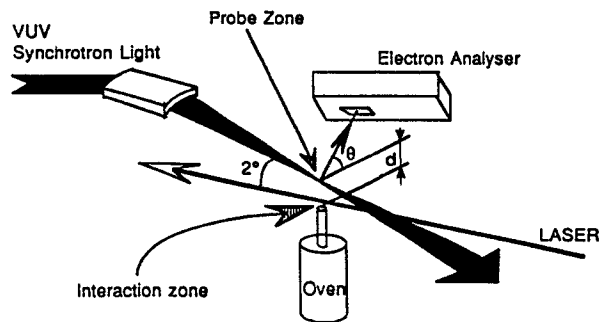


FIG. 2. Schematics of the experimental setup. The distance d between the interaction zone and the probe zone amounts to about 3 mm. $\Theta = 54.7^\circ$, as measured with respect to the polarization vector of the vuv photon beam.

by a narrow effusive jet of gas obtained from a very thin needle (0.3 mm in diameter) issued from an oven heated gently to about 80 °C, crossing at right angles the laser beam originating from a cw argon ion laser, used in a multiline mode mostly, 476.5, 488, 496.5, 501.7, 514.5, and 528.7 nm with 6%, 32%, 6%, 10%, 22%, and 10% of the total intensity, respectively. Because the laser beam is carried through different mirrors with different planes of reflection, the original polarization of the laser is lost, and there is no preferential orientation of the photoexcited molecule. The vuv beam actually crosses the region at a point located only 3 mm away from the laser/gas interaction point. Photoelectrons are energy selected in a 127° cylindrical electrostatic analyzer, which is used at low (electron energy bandwidth FWHM, $\Delta E = 180$ meV) or medium ($\Delta E = 120$ meV) resolution, the latter being necessary to resolve stretching modes. Under these conditions, owing to the high particle density inside the oven and the ability of this compound to polymerize, *s*-tetrazine exhibits a strong explosive character which has prevented us from running the experiment for long periods of time.

The arrangement shown in Fig. 2 is somewhat different from the one used in our previous studies.^{15,16} Here both photon beams are (nearly) collinear, and no longer perpendicular. The small angle (2°) between both photon beams, in the vertical plane, prevents the laser light to damage the refocusing mirror of the synchrotron light beam. This new geometry, allows us to position the electron analyzer at a selected angle with respect to the polarization vector of the incident vuv photon beam of 54.7° , thus eliminating possible angular effects.

The laser power was set at a minimum value of 3 W in the chamber, to obtain a nearly full dissociation. Note that under these conditions, only one photon transitions have to be considered.

s-tetrazine has been produced using the method described by Marcellis and van der Plas,¹⁸ which offers the advantage over the original synthesis of Spencer *et al.*,¹⁹ that there is no pyrolytic decarbonylation step. Purity was carefully checked by mass spectrometry, infrared and visible spectrometry.

All photoelectron spectra have been corrected for the transmission of the analyzer. The partial pressure and light flux were controlled to be constant during data acquisition period (typically 15 mn).

III. RESULTS AND DISCUSSION

A. Nature of the fragments and yield

We present in Fig. 3(a) the photoelectron spectrum of *s*-tetrazine, laser off, recorded at 23 eV photon energy and with a total bandwidth of 190 meV. As mentioned in Sec. II, this energy offers the best conditions of sensitivity for detecting the fragments. The bands (including the strong one located around 20 eV binding energy, not fully shown in the figure), correspond to the valence ionization spectrum, in excellent agreement with the best data available at this time.^{20,21} The detailed assignment has been made by von Niessen *et al.*²² on the basis of many body Green's function calculations. No further comments will be made at this point since it is out of the scope of this paper.

When the laser is turned on with a power of 3 W in the chamber, the spectrum changes drastically, as seen in Fig. 3(b) because of the nearly complete dissociation of the parent molecule. The laser is used here in a multiline mode. The various wavelengths correspond to the $S_0 \rightarrow S_1$ transition with excess energies with respect to the 0-0 band, equal to 787, 1308, 1804, 2013, 2364, and 2858 cm^{-1} , respectively. None of them matches an intense line of the photoabsorption spectrum.^{19,23} The 528.7 nm light falls in the rotational tail of the $6b_0^2$ line (2 cm^{-1} above), the 514.5 nm light lies at 52

cm^{-1} above the $6_0^2 16a_2^2$ line, the 501.7 nm light lies 23 cm^{-1} above the $6a_0^1 16b_0^1 17b_0^1$ line, the 496.5 nm light lies 51 cm^{-1} above the $6a_0^3 16a_2^2$ line and the 488 nm light lies 106 cm^{-1} above $6a_0^3 16b_1^1$, the 476.5 nm light lies 63 cm^{-1} above the $6a_0^4$ line. From the work of Innes *et al.*,²³ those lines correspond essentially to the excitation of in-plane breathing modes of the ring. We have reported in Table I the useful structural elements and the vibrational frequencies as measured for the parent molecule^{19,23,24} and fragments.²⁵⁻²⁷

In Fig. 3(b), all the bands are readily interpreted as due to HCN and N_2 . They correspond to the well known X , A , and B bands of N_2^+ (see, e.g., Ref. 28) and the \tilde{X} , \tilde{A} , and \tilde{B} bands of HCN^+ .²⁹ There is a small residual signal of the parent molecule but the overlap of the *s*-tetrazine bands and those of the fragments is negligible except for the \tilde{B} state of HCN^+ . The main information brought by this spectrum is that there is no signal due to any fragments like HCNN_2 or HCNNCH , which have been proposed in stepwise processes (2) or (3). Indeed, the first ionization potential of any isomeric form of $\text{H}_2\text{C}_2\text{N}_2$ lies around 10 to 11 eV^{30,31} and should have been detected in the present experiment, as long as its lifetime would have been longer than a few 100 ns, the dead time of our detection technique.

The relative intensity I of each resolved band, labeled i for HCN and j for N_2 is proportional to the partial photoionization cross section, σ , at 23 eV photon energy, and the stoichiometric factor β of the photodissociation cross section. One can thus write

$$I(\text{HCN}_i)/I(\text{N}_2_j) = \beta\sigma(\text{HCN}_i)/\sigma(\text{N}_2_j).$$

The value of $\sigma(\text{N}_2)$ for the X state of N_2^+ is known³² at this specific energy as 9.4 Mb. For the HCN molecule, there is no experimental data available. Only theoretical values³³ have been published to our knowledge. The relative intensity of each i and j bands is reported in Table II. Taking the β factor equal to 2, we readily extract from the relative intensity of the bands, the partial absolute photoionization cross section for HCN, i.e., 13.5 Mb the sum of \tilde{X} and \tilde{A} state, 3.6 Mb for the \tilde{B} state, by normalization to the X state of N_2^+ . These values compare favorably with the calculations of 12.8 Mb for the $\tilde{X} + \tilde{A}$ states and 10 Mb for the \tilde{B} state,³³ at 23 eV photon energy. This shows that there is a reasonable accord with theory. Moreover, this method provides easily absolute photoionization cross section of fragment species as soon as the cross section for one of the other fragment is known.

B. Vibrational distribution in the fragments

We turn now to the analysis of the vibrational bands of the fragments. We have used an improved electron energy resolution (130 meV in total) in order to resolve stretching modes. The corresponding spectra of nascent N_2 and of nascent HCN are shown in Figs. 4 and 5, respectively. Note that the small contribution of the *s*-tetrazine bands has been subtracted. This does not affect the fragment bands of interest because there is no overlap, except around 20 eV binding energy. Indeed, unlike the other fragment bands, the shape of the \tilde{B} band of HCN^+ cannot be taken on quantitative grounds. This is why we will focus here on the \tilde{X} and \tilde{A} states of HCN.

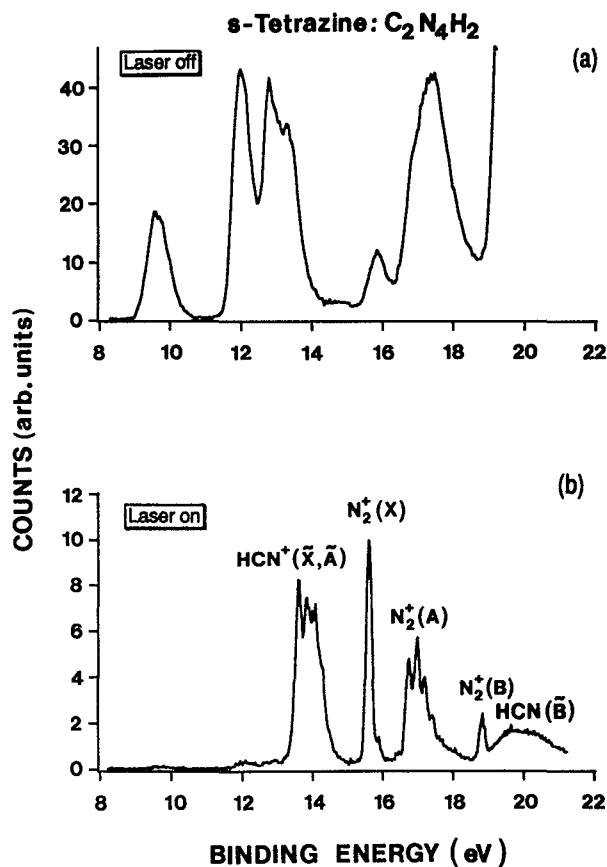


FIG. 3. Photoelectron spectrum of *s*-tetrazine recorded at 23 eV photon energy (synchrotron radiation) and 0.19 eV total energy resolution (a) laser off, (b) laser on (3 W).

TABLE I. Geometrical parameters and useful vibrational frequencies of *s*-tetrazine, HCN, and N₂.

Geometry	<i>s</i> -tetrazine (Refs. 19,23,24)	HCN (Ref. 26)	N ₂ (Ref. 25)
C–H distance (Å)	1.06	1.064	...
C–N distance (Å)	1.33	1.156	...
N–N distance (Å)	1.32	...	1.094
HCN angle (°)	116	180	...
Vibrational frequency (cm ⁻¹)	C ₂ N ₄ H ₂ , S ₀ ¹ A _g (Ref. 23) ν _{oo} (a _g):736.1 ν _{oa} (a _g):1526.2 ν _{ob} (b _{3g}):651.1	HCN, $\tilde{X}^1\Sigma^+$ (Ref. 26) ν ₁ :3311.47 ν ₂ :713.46 ν ₃ :2096.7	N ₂ , $X^1\Sigma_g^+$ (Ref. 25) ω _c = 2359.61

Let us first analyze, the nitrogen signal. The direct evidence of vibrationally hot molecules is seen by the existence of the hot line N₂⁺ X¹Σ_g⁺, ν = 1 → N₂⁺ A²Π_u, ν = 0 (1 → 0 in a simplified form) located at a binding energy of 16.43 eV. The energy separation between this line and the regular (X¹Σ_g⁺, ν = 0 → A²Π_u, ν = 0) line, (0 → 0), equals 0.293 ± 0.05 eV, which matches exactly the first ν = 0, 1 energy separation of the ground state of the neutral molecule, i.e., 0.291 eV (Ref. 25). Note that there is no signal corresponding to the (2 → 0) line within the limit of our background noise, at 16.14 eV binding energy. The observation of such hot bands in the A state is possible because the potential curve is such that the FC (Franck–Condon) factors F₁₋₀ is large, i.e., 0.38.³⁴ We readily extract the vibrational population of the nascent nitrogen fragment (see Table III), i.e., 94.6% for ν = 0 and 5.4% ± 0.5% for ν = 1.

Let us consider the HCN signal. Unlike nitrogen, we do not resolve the full vibrational structure because of our limited resolution. The peak energies result from a calibration of the binding energy scale made at the N₂⁺, X²Σ_g⁺ ν = 0 position. We have compared it to the contour of “vibrationally cold” HCN, as established at room temperature, from Fridh and Åsbrink,²⁹ using very high resolution photoelectron spectroscopy. In order to make a meaningful comparison, we convoluted their spectrum with our experimental resolution, i.e., 130 eV, precisely measured from the FWHM of the N₂ vibrational bands. The corresponding profile is shown in Fig. 5 as a dashed line. We observe that there is a marked difference, showing that nascent HCN is surely vibrationally

excited. In order to analyze the “hot” component, and correctly subtract the “cold” part, we have made the assumption that 000 → 000 peak (\tilde{X} state) is only due to cold HCN. Then after normalizing both spectra at this particular binding energy, i.e., 13.607 eV, we obtain the “difference” spectrum as shown in Fig. 5. This difference spectrum is surprisingly intense and markedly structured and show four main features labeled *A*, *B*, and *C* in Fig. 5(b).

The analysis of the difference spectrum requires a detailed knowledge of the vibrational spectroscopy of the \tilde{X} and \tilde{A} states of HCN⁺. Apart from the original work of Fridh and Åsbrink²⁹ which offers a detailed assignment of the photoelectron spectrum based on classical spectroscopy, Köppel *et al.*³⁵ have made a successful quantitative interpretation in introducing non Born–Oppenheimer effects. They have shown that vibronic coupling between the $\tilde{X}^2\Pi$ and $\tilde{A}^2\Sigma^+$ states of HCN⁺, leads to a perturbation of the spectrum, especially above 14 eV binding energy. The strong mixing manifests itself by an intricate interplay between the bending (ν₂) and C–N stretching (ν₃) modes (the C–H stretching mode, ν₁ can be ignored). According to Köppel *et al.*,³⁵ the PES lines located below 13.95 eV can be described essentially with vibrational progressions of the pure \tilde{X} state. In contrast, above 13.95 eV, the mixture of states is such that

TABLE II. Absolute photoionization cross section of HCN and N₂, at 23 eV photon energy.

Band	Relative intensity (arb. units)	Partial photoionization cross section (Mb)
HCN ⁺ (\tilde{X} + \tilde{A})	201	13.5
HCN ⁺ (\tilde{B})	53	3.6
N ₂ ⁺ (X)	70	9.4*
N ₂ ⁺ (A)	105	14.1
N ₂ ⁺ (B)	15	2.0

*Normalized to the value of Ref. 32.

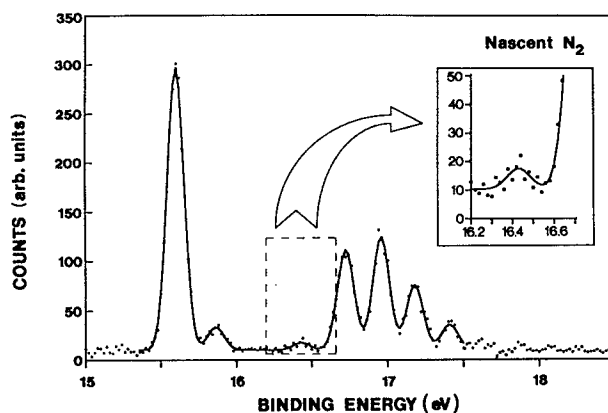


FIG. 4. Photoelectron spectrum of nascent N₂ fragment (X and A bands) recorded with 23 eV synchrotron radiation and 0.13 eV total energy resolution and laser on (3 W).

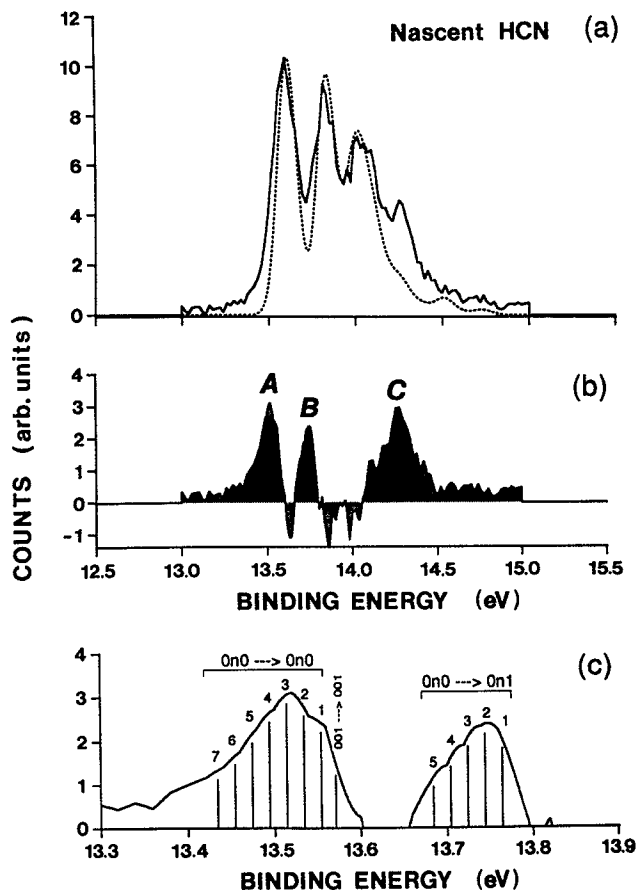


FIG. 5. (a), solid line. Photoelectron spectrum of nascent HCN fragment (\tilde{X} and \tilde{A} bands) recorded with 23 eV synchrotron radiation and 0.13 eV total energy resolution and laser on (3 W). Top, dashed line. Photoelectron spectrum of cold HCN from Ref. 29, convoluted with our present energy resolution. (b), Difference spectrum between the nascent and cold spectra with details of the A and B bands in (c).

it is not possible to assign any line to one pure \tilde{X} or \tilde{A} electronic state. We readily see that the \mathcal{A} and \mathcal{B} features belong to the unperturbed part of the spectrum, whereas \mathcal{C} belongs to the complex part.

We interpret the \mathcal{A} and \mathcal{B} bands as due primarily to hot bands due to bending excitation of the nascent fragment, because of the following. Fridh and Åsbrink²⁹ have observed two hot bands in the HCN PES spectrum located at 13.554 eV ($01^10 \rightarrow 010$) and 13.764 eV ($01^10 \rightarrow 011$). From their analysis, 6% of HCN at room temperature is found in $\nu_2 = 1$. We readily extract from the relative intensity of two hot bands, as measured in Ref. 29, that the transition probabilities are 0.3 and 0.15, respectively. Since both bands are the only one observed, we consider that the corresponding transitions have the most favorable FC factors, in agreement with the selection rules of Dixon *et al.*,³⁶ i.e., in the present case, $\Delta\nu_2 = 0$, $\Delta\nu_3 = 0, 1$, and used in Ref. 29. These two hot lines coincide in energy respectively with the high energy edges of the \mathcal{A} and \mathcal{B} bands. We believe that other hot lines are also present. Since the bending frequency is smaller by 20 meV (160 cm^{-1})^{3,4} in the ion state compared to the neutral molecule, we expect the ($0n0 \rightarrow 0n0$) and ($0n0 \rightarrow 0n1$) bend-

TABLE III. Vibrational distribution in the neutral fragments.

Nascent N_2 fragment	
$\nu = 0$	$94.6 \pm 0.5\%$
$\nu = 1$	$5.4 \pm 0.5\%$
HCN fragment	
Bending	
(000)	70%
($0n0$) $n = 1$ to 6	26%
Estimated partitioning	
(010)	3%
(020)	5%
(030)	7%
(040)	6%
(050)	3%
(060)	2%
C–N stretching	
001	<4%

ing progressions associated, respectively, to $\nu_3 = 0$ and 1, to lie on the low energy side of the first hot transition. We have then obtained that the \mathcal{A} band is likely made of some six lines, the maximum of the band being found for $\nu_2 = 3$. Assuming the same transition probability for the first hot line ($01^10 \rightarrow 010$) as for the others, we obtain that the total probability for bending excitation (six levels), $\Sigma\alpha_n$ (bending) is given by

$$I_A = \frac{I_0}{F_0(1 - \Sigma\alpha_n)} \Sigma I_n,$$

with $I_n = \alpha_n F_{n-n}$, where I_A represents the total intensity of the \mathcal{A} band, I_0 the intensity of the main 000 band of the \tilde{X} state, F_{n-n} the Franck–Condon (FC) factor for the Δn (ν_2) = 0 transition, and F_0 the FC factor for the main transition. Assuming a constant value for $F_{n-n} = 0.3$ and $F_0 \sim 0.36$ as estimated from the work of Ref. 29, we obtain

$$\Sigma\alpha_n / (1 - \Sigma\alpha_n) = I_A F_0 / I_0 F_{n-n}.$$

We measure from the results of Fig. 5, $I_A/I_0 = 0.3$ and we obtain $\Sigma\alpha_n / (1 - \Sigma\alpha_n) = 0.3 \times F_0 / F_{n-n}$. Assuming $F_0/F_{n-n} = 1.2$, we obtain $\Sigma\alpha_n = 0.265$. Knowing the energy separation of individual hot lines, we have estimated the distribution of Fig. 6 and Table III to obtain a reasonable fit with the \mathcal{A} band. For the \mathcal{B} band, we proceed along the same lines as for the \mathcal{A} band and we find that the information is consistent with a bending excitation as reported in Table III.

We observe also that the \mathcal{B} band is narrower than the \mathcal{A} band. It is possible that \mathcal{A} contains another hot line, i.e., the $001 \rightarrow 001$ transition. We expect this line to lie 37 meV below the main 000 line of the \tilde{X} state. This position lies on the high energy edge of the \mathcal{A} band. According to the potential curve of the ionic state,³⁵ we expect that the FC factor is rather large since the equilibrium distance of the \tilde{X} state equals 1.21 Å, i.e., 0.06 Å larger than the neutral molecule. Consequently, we offer to consider the existence of such line, with an intensity not higher than the \mathcal{A} band intensity at the nominal energy (– 37 meV), taking into account our present energy resolution

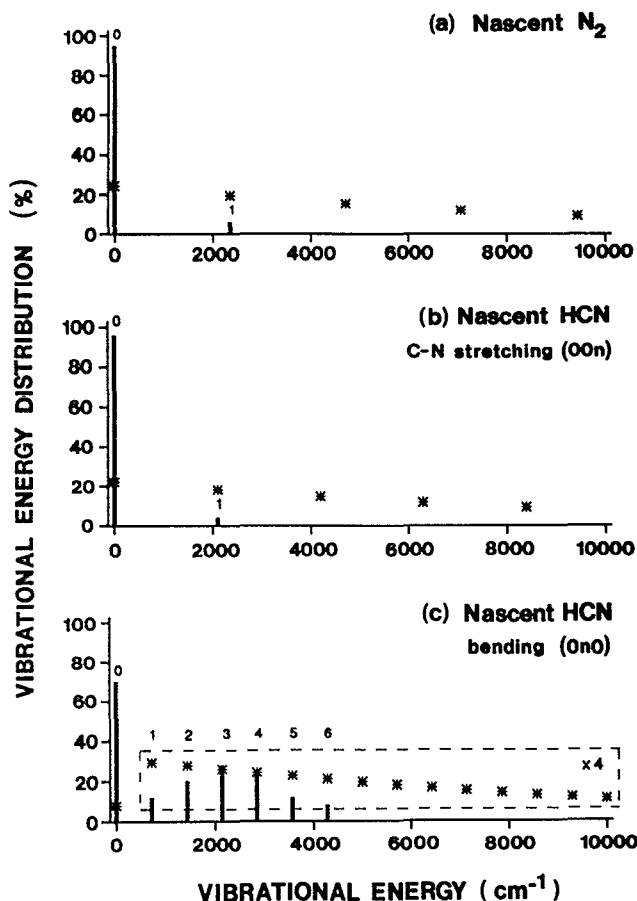


FIG. 6. Vibrational energy distributions α_n for nascent N_2 and HCN fragments (bars), as evaluated from this work. Vibrational energy distributions expected in a pure statistical model (stars).

$I(\text{C-N stretching})$

$$= I_0 \frac{\alpha_1}{1 - \alpha_1} (\text{C-N stretching}) F_{1-1} / F_0.$$

We estimate the ratio $I(\text{C-N stretching})/I_0 < 0.05$. Taking $F_{1-1}/F_0 \sim 1$, we obtain an estimated value of α_1 (C-N stretching) smaller than 0.05. The results are reported in Fig. 6 and Table III.

The vibrational energy distributions of the nascent N_2 and HCN, reported in Table III, are reported in Fig. 6 for comparison with a statistical theoretical model (see Sec. III C). The fact that these fragments are relatively cold in the stretching modes is in agreement with the work of Coulter *et al.*⁵ They report 1% for one quantum of ν_3 in HCN and estimate some 10% in $\nu = 1$ in N_2 . No comparison can be made for the bending modes of HCN, which have never been probed directly to our knowledge.

We now deduce the maximum energy devoted to vibration. It amounts to the sum of $\nu = 1$ (N_2) plus twice the sum of the frequency of 001 and 060, for HCN. We obtain $0.3 + 2(0.26 + 0.089 \times 6) = 1.88$ eV (43.35 kcal/mol). We also see that the maximum of the vibrational distribution corresponds to an average value of 0.188 eV (4.335 kcal/mol), i.e., 0.054 quanta in N_2 , 0.04 quanta of ν_3 , and 0.85 quanta of ν_2 . Those numbers are significantly smaller than

those deduced from the translational energy distribution of Zhao *et al.*⁷ According to this previous work, when *s*-tetrazine is photoexcited at the S_1 (0-0) level, the total translational energy amounts to 73.9% of the total available energy, i.e., 80.7 kcal/mol. Zhao *et al.* observe also that any excess energy in S_1 is found as translational energy. In other words, the fragments are found with essentially the same internal energy, independently of the energy deposited in S_1 . We deduce then from this previous work, that the fragments carry 28.5 kcal/mol (1.26 eV) internal energy. The difference with our results amounts to 24.2 kcal/mol. Apart from the uncertainty in this work (i.e., error bars of the intensity of $\nu = 1$ for N_2 , the error bar for the intensity and distribution of bending and C-N stretching in HCN) and in Ref. 7, part of this gap is probably due to rotation. This point is discussed in the next section.

C. Dynamics of the dissociation process

From the present data, we cannot conclude directly that we observe a concerted three body fragmentation because the dead time (100 ns) of our experiment is too long compared to the relevant time scale of the process. However, the internal energy distribution of the fragments can be analyzed in more details and related to different dynamical models. We find that the fragments are almost totally vibrationally cold, in the N_2 and CN (in HCN) stretching motion and rather hot in the HCN bending motion. In a pure statistical redistribution of this available energy, we would have expected a large fraction of it to be found in internal energy of the fragments, because the available energy is very large and amounts to the minimum value of S_1 (0-0), i.e., 109.2 kcal/mol (4.77 eV). Such vibrational distribution is evaluated as follows. Considering the $(\text{HCN})_2 \cdots N_2$ system, the level density ρ is given by

$$\rho = k / [E_T - E(\text{HCN})_2 - E(N_2)]^{1/2},$$

where k is a constant. We have $E(\text{HCN})_2 = E(\text{HCN}) + E(\text{HCN}) + \epsilon$, with ϵ being the translational energy for the $\text{HCN} \cdots \text{HCN}$ separation. Integrating ρ four times (one for translation and three for rotation, which correspond to coordinates undetermined in our experiment) of the three fragments, we obtain

$$\langle \rho \rangle = [E_T - E_{\text{HCN}}^{\text{vib}} - E_{\text{HCN}'}^{\text{vib}} - E_{N_2}^{\text{vib}}]^{7/2}.$$

Here we only consider the ν_2 and ν_3 modes for HCN. The ρ values for each of the relevant vibrational modes of the fragments are reported in Fig. 6. Indeed, the observed distributions depart strongly from the statistical model. A similar conclusion has been found by Zhao *et al.*⁷ using translational energy distribution measurements. In addition, they have established that the fragmentation is governed by the repulsive shape of the potential surface in the exit channels (N-N and the two C-N reactions coordinates). We find the same qualitative conclusion, since we confirm that very little internal energy is left for the fragments. However, the detailed energy distribution of the fragments shed some light on the "perpendicular coordinates" which oppose themselves to the reaction coordinates. They are the remaining N-N and C-N stretching, and $\widehat{\text{HCN}}$ angle which are clearly

visualized in the activated complex calculated by Scheiner *et al.*⁸ and reported in Fig. 7. This transition state corresponds to the top of the barrier shown in Fig. 1, positioned at 47 kcal/mol. We have reported in the same figure, the potential energy curves of N₂ and HCN (C–N stretching and bending) as well known from the literature.^{37–39} We readily see that the perpendicular coordinates in the transition state are very close to the equilibrium distances N–N and C–N in the N₂ and HCN molecules. These differences amount to $\Delta R(\text{N–N}) = 0.05 \text{ \AA}$ and $\Delta R(\text{C–N}) = 0.03 \text{ \AA}$. From the potential curves of Fig. 7, we see that the corresponding stretching maximum amplitude matches barely $\nu_3 \sim 0$ in HCN and $\nu = 1$ in N₂. The very small stretching excitation in the fragments is fully compatible with the distances calculated in the transition state. Notice that in the neutral ground state *s*-tetrazine molecule, the same distances are much larger (see Table I) than in the fragments. If this initial geometry would have played a role in the energy content of the fragments, we would have seen a very large vibrational energy content in the stretching modes, as expected from the poten-

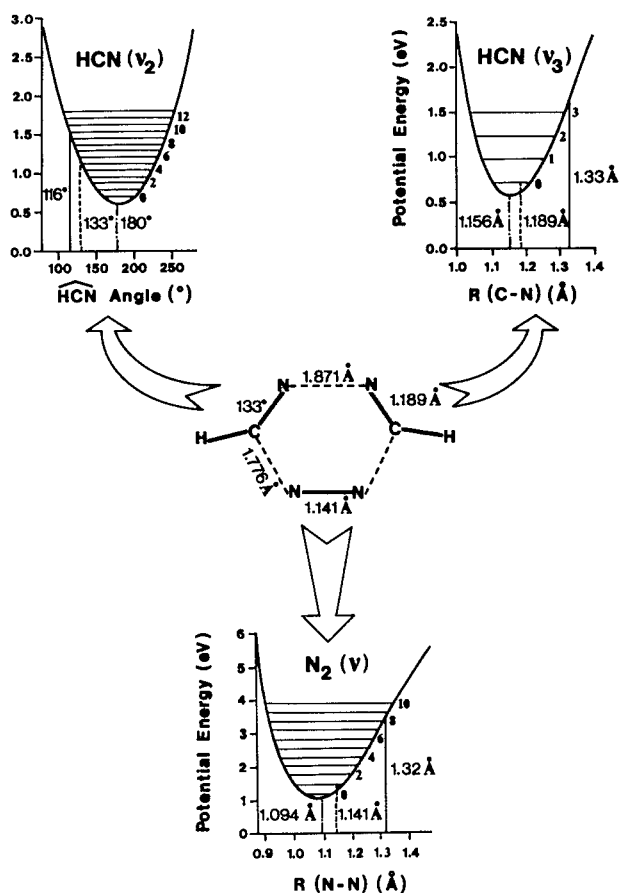


FIG. 7. Transition state for the unimolecular triple dissociation of *s*-tetrazine as calculated in Ref. 8 and its relevance to the vibrational excitation of the fragments within the equilibrium geometry model. The potential energy curves of N₂ and HCN (C–N stretching and bending) as calculated in Refs. 37–39 and the relevant equilibrium coordinates for the ground state molecule, transition state, and fragments (dashed vertical lines) provides the maximum of the distribution (see the text).

tial curves of Fig. 7. This is evidently not the case. Turning now to the bending motion, we see that the HCN angle in the transition state amounts to 133°, i.e., a difference of 47° with the equilibrium geometry in HCN. According to the potential along the bending coordinate, the angle amplitude corresponds to a maximum of $\nu_2 = 5$. This is consistent with our findings. Again this means that the geometry of the transition state, and especially the atomic distances and angles which are not active in the dissociation channel, is ruling the vibrational energy content of the fragments. We believe that this nice situation is favored because of the small excess energy ($< 0.46 \text{ eV}$) of the *S*₁ state with respect to the top of the barrier (Fig. 1) at which the geometry of the transition state has been calculated. We conclude that the unimolecular photodissociation of *s*-tetrazine can be well described by the equilibrium geometry model, introduced by Mitchell and Simons⁴⁰ for interpreting the photodissociation of triatomic molecules into one atom and a vibrationally excited molecular fragment. The difference, here, is twofold: (i) the extension of this model to a three body photodissociation process. This requires that the three bonds break simultaneously, as expected in a concerted mechanism, (ii) the fact that the interatomic distances in the perpendicular coordinates, in the transition state, are smaller than in the neutral molecule, in contrast to the original triatomic systems.

We have seen in Sec. III B that the fragments may carry rotational energy because the translational energy obtained by Zhao *et al.*,⁷ measured at the maximum of the distribution is not sufficient to explain the total available energy. If this is the case the amount of rotational energy is very large, i.e., a most probable value of 24.2 kcal/mol. We believe that the two HCN fragments are carrying a large part of this energy, because Zhao *et al.*⁷ have shown, on the basis of angular anisotropy in this fragmentation, that there is a stronger repulsion between both HCN fragments than between one HCN and N₂. If it is so, it is reasonable to find up to several kcal/mol rotational energy per HCN fragment and much less in N₂. In other words, there would be a strong coupling between rotation and translation in the dynamics of the process, having in mind that vibration is uncoupled to the former. Note that such prediction is intimately related to the accuracy of the present data and those of Ref. 7 and requires either direct probe on HCN rotation or improved measurements on the vibrational distributions.

IV. CONCLUSIONS

Photoelectron spectroscopy with synchrotron radiation has been proved to be an efficient method to probe simultaneously HCN and N₂ nascent fragments issued from the photodissociation of *s*-tetrazine in the *S*₁ state. More importantly, vibrational energy distributions of both N₂ and HCN could be probed directly. Despite the lack of energy resolution to resolve hot bands for HCN we have shown the presence of a very little stretching excitation in both N₂ and HCN and a large amount in bending motion of HCN. The maximum of the distribution is found fully compatible with the “perpendicular coordinates” of the transition state calculated by *ab initio* molecular structure calculations. We thus conclude that the unimolecular dissociation of *s*-tetra-

zine can be well described by the equilibrium geometry model. The geometry of the transition state calculated by *ab initio* quantum chemical calculations, being associated to a concerted three body mechanism, our findings are consistent with this model. Extension of this work with higher energy resolution in the detection is needed to provide more accurate numbers and confirm our prediction of large amounts of rotation especially in the two HCN fragments.

ACKNOWLEDGMENTS

We are very grateful to Professor J. A. Beswick (LURE, Orsay), Dr. B. Soep (Laboratoire de Photophysique moléculaire, Orsay), and Dr. P. Millié (DRECAM/SPAM, Saclay) for very helpful discussions on photodissociation dynamics. We warmly thank M. Plisnier and Professor Flammang from the Mons University in Belgium, as well as M. Henry (C. E. N. Saclay) for synthesizing the *s*-tetrazine in large quantities through a long and tedious procedure. We are very grateful to J. L. Maréchal (C. E. N. Saclay, France) for his efficient technical support and to the LURE staff for operating the Super ACO storage ring. This work has been supported by contract CEA/XRS No. SA 8176/BJ.

¹ T. Curtius, A. Darapsky, and F. Müller, *Chem. Ber.* **40**, 84 (1907).

² J. Koenigsberger and K. Vogt, *Phys. Z.* **14**, 1269 (1913).

³ R. M. Hochstrasser and D. S. King, *J. Am. Chem. Soc.* **97**, 4760 (1975).

⁴ D. M. Burland, F. Carmona, and J. Pacansky, *Chem. Phys. Lett.* **56**, 221 (1978).

⁵ D. Coulter, D. Dows, H. Reisler, and C. Wittig, *Chem. Phys.* **32**, 429 (1978).

⁶ J. H. Glowina and S. J. Riley, *Chem. Phys. Lett.* **71**, 429 (1980).

⁷ X. Zhao, W. B. Miller, E. J. Hints, and Y. T. Lee, *J. Chem. Phys.* **90**, 5527 (1989).

⁸ A. C. Scheiner, G. E. Scuseria, and H. F. Schaefer III, *J. Am. Chem. Soc.* **108**, 8160 (1986).

⁹ C. E. M. Strauss and P. L. Houston, *J. Phys. Chem.* **94**, 8751 (1990).

¹⁰ J. Baker, M. Barnes, M. C. R. Cockett, J. M. Dyke, A. M. Ellis, M. Fehre, E. P. F. Lee, A. Morris, and H. Zamanpour, *J. Electron Spectrom. Relat. Phenom.* **51**, 487 (1990).

¹¹ K. Kimura, *Photoelectron Spectra of Unstable Species* (Institute for Molecular Sciences, Okasaki, 1989); Internal report (unpublished).

¹² M. C. R. Cockett, J. M. Dyke, A. M. Ellis, M. Fehre, and T. G. Wright, *J. Electron Spectrom. Relat. Phenom.* **51**, 529 (1990).

¹³ H. Bock and R. Dammel, *Angew. Chem. Int. Ed. Engl.* **26**, 504 (1987).

¹⁴ The original idea of coupling laser and synchrotron radiation to solve this problem was suggested to us by Professor A. H. Zewail (Caltech, Pasadena) in the course of collaboration at LURE.

¹⁵ L. Nahon, J. Tremblay, M. Larzillière, L. Duffy, and P. Morin, *Nucl. Inst. Methods B* **47**, 72 (1990).

¹⁶ L. Nahon, L. Duffy, P. Morin, F. Combet-Farnoux, J. Tremblay, and M. Larzillière, *Phys. Rev. A* **41**, 4879 (1990); L. Nahon, A. Swensson, and P. Morin, *ibid.* **43**, 2328 (1991).

¹⁷ P. R. Woodruff and G. V. Marr, *Proc. R. Soc. London, Ser. A* **358**, 87 (1977).

¹⁸ A. T. M. Marcelis and H. C. van der Plas, *J. Heterocyclic Chem.* **24**, 545 (1987).

¹⁹ G. H. Spencer, Jr., P. C. Cross, and K. B. Wiberg, *J. Chem. Phys.* **35**, 1925, 1939 (1961).

²⁰ C. Fridh, L. Åsbrink, B. O. Jonsson, and E. Lindholm, *Int. J. Mass Spectrom. Ion Phys.* **9**, 485 (1972).

²¹ R. Gleiter, E. Heilbronner, and V. Hornung, *Helv. Chim. Acta* **55**, 255 (1972).

²² W. von Niessen, W. P. Kraemer, and G. H. F. Dierksen, *Chem. Phys.* **41**, 113 (1979).

²³ K. K. Innes, L. A. Franks, A. J. Merer, G. K. Vemulapalli, and T. Cassen, J. Lowry, *J. Mol. Spectrosc.* **66**, 465 (1977).

²⁴ A. J. Merer and K. K. Innes, *Proc. R. Soc. A* **302**, 271 (1968).

²⁵ G. Herzberg, *Molecular Spectra and Molecular Structure I, Spectra of Diatomic Molecules* (Van Nostrand, New York, 1950).

²⁶ G. Herzberg, *Molecular Spectra and Molecular Structure III, Molecular Spectra and Molecular Structure of Polyatomic Molecules* (Van Nostrand, Princeton, 1966).

²⁷ A. M. Smith, S. L. Coy, W. Klemperer, and K. K. Lehmann, *J. Mol. Spectrosc.* **134**, 134 (1989).

²⁸ K. Kimura, S. Katsumata, Y. Achiba, T. Yamazaki, and S. Iwata, *Handbook of Photoelectron Spectra of Fundamental Organic Molecules* (Japan Scientific Societies, Tokyo, 1981).

²⁹ C. Fridh and L. Åsbrink, *J. Electron Spectrom. Relat. Phenom.* **7**, 119 (1975).

³⁰ O. I. Osman and H. W. Kroto (private communication, 1987).

³¹ I. Nenner, O. Dutuit, M. Richard-Viard, P. Morin, and A. H. Zewail, *J. Am. Chem. Soc.* **110**, 1093 (1988).

³² P. Lablanquie, Thèse de 3ème cycle, Orsay, 1984. Rapport CEA-R-5295 (1985).

³³ J. Kreile, A. Schweig, and W. Thiel, *Chem. Phys. Lett.* **87**, 473 (1982).

³⁴ H. Lefebvre-Brion (private communication).

³⁵ H. Köppel, W. Domcke, and L. S. Cederbaum, *Adv. Chem. Phys.* **57**, 59 (1984).

³⁶ R. N. Dixon, G. Duxbury, M. Horani, and J. Rostas, *Mol. Phys.* **22**, 977 (1971).

³⁷ A. Lofthus and P. H. Krupenie, *J. Phys. Chem. Ref. Data* **6**, 113 (1977).

³⁸ J. M. Murrell, S. Carter, and L. O. Halonen, *J. Mol. Spectrosc.* **93**, 307 (1982).

³⁹ P. K. Pearson and H. F. Schaefer III, *J. Chem. Phys.* **62**, 350 (1975).

⁴⁰ R. C. Mitchell and J. P. Simons, *Discuss. Faraday Soc.* **44**, 208 (1967).